NASA Contractor Report 182040
ICASE Report No. 90-35

AD-A227 363

ICASE

FOURIER ANALYSIS OF FINITE ELEMENT
PRECONDITIONED COLLOCATION SCHEMES

Michel O. Deville
Ernest H. Mund

DTIC
S ELECTE D
OCT 03 1990
E

DISTRIBUTION STATEMENT A
Approved for public release;
Distribution Unlimited

NASA
National Aeronautics and
Space Administration

Langley Research Center
Hampton, Virginia 23665-5225

90 10 03 055

FOURIER ANALYSIS OF FINITE ELEMENT PRECONDITIONED COLLOCATION SCHEMES

Michel O. Deville[1]
Université Catholique de Louvain
Unité de Mécanique Appliquée
Louvain-La-Neuve, Belgium

and

Ernest H. Mund
Université Libre de Bruxelles
Service de Métrologie Nucléaire
Bruxelles, Belgium
and
Université Catholique de Louvain
Unité de Thermodynamique et Turbomachines
Louvain-La-Neuve, Belgium

Accession For

NTIS GRA&I

DTIC TAB

Unannounced

Justification

By

Distribution/

Availability Codes

Dist | Avail and/or Special

A-1

ABSTRACT

This paper investigates the spectrum of the iteration operator of some finite element preconditioned Fourier collocation schemes. The first part of the paper analyses one-dimensional elliptic and hyperbolic model problems and the advection-diffusion equation. Analytical expressions of the eigenvalues are obtained with use of symbolic computation. The second part of the paper considers the set of one-dimensional differential equations resulting from Fourier analysis (in the tranverse direction) of the 2-D Stokes problem. All results agree with previous conclusions on the numerical efficiency of finite element preconditioning schemes.

i

1. INTRODUCTION

In the recent past, Chebyshev collocation schemes have been applied extensively to the numerical integration of the Navier-Stokes equations [1, 3, 4]. For scalar elliptic problems, it is well known that the condition number of the matrix system of discrete algebraic equations increases rapidly with N, the number of degrees of freedom of the problem at hand. Therefore, the preconditioning technique seems to be the only adequate tool in order to overcome this numerical burden. The present authors [5, 6] demonstrated that finite elements (FE) constitute powerful preconditioners for general second-order elliptic equations. In [3], several fluid flow elements in velocity-pressure formulation were investigated. From the analysis of the eigenspectrum of the iteration operator, it was shown that the Q2-Q1 element is the best choice for the steady Stokes problem. As all the previous analyses on finite element preconditioning were carried out numerically, the present note aims at analytical results through use of symbolic manipulation languages (cfr. [10]).

For the sake of simplicity, we will restrict ourselves to the study of a finite element preconditioned Fourier collocation scheme. In this case, the mesh size is uniform and the algebra is considerably reduced. In Section 2, a one-dimensional model is considered. The collocation process is preconditioned by Lagrangian linear, quadratic, cubic and Hermite cubic elements, respectively. The Richardson iteration method is set up with these FE preconditioners as approximate operators and algebraic solvers. Using the spatial structure of the eigenvectors of the Fourier solutions, one may perform a full analysis of the eigenvalues of the iteration operator. This theoretical investigation corroborates the previous numerical analyses [6]. In Section 3, a one-dimensional hyperbolic model is investigated using linear and quadratic FE preconditioning. The upwinding technique is also examined. A further model consists in an advection-diffusion equation. In Section 4, the Stokes problem is reduced to a 1-D incompressible flow model amenable to Fourier discretization. The Q2-Q1 and Q1-P0 elements are candidates as preconditioners. A similar Fourier analysis is done. The results corroborate numerical experiments carried out in the framework of Chebyshev collocation [3].

2. ELLIPTIC MODEL

Let us first consider the simple elliptic problem:

$$-u_{xx} = f, \qquad 0 \leq x \leq 2\pi, \qquad (2.1)$$

with periodic boundary conditions. The subscript indicates partial derivative. The Fourier approximation of the dependent variable u is

$$u_N = \sum_{p=-N/2}^{N/2-1} \hat{u}_p e^{ipx_j}, \qquad 0 \leq j < N, \qquad (2.2)$$

where $\hat{u}_p$ are the discrete Fourier coefficients and x_j the collocation points defined by

$$x_j = \frac{2\pi j}{N}, \qquad j \in [0, N[. \qquad (2.3)$$

1

The linear system corresponding to (2.1) may be found in [1] and will be denoted by L_c. The eigenfunctions of (2.1) are

$$\xi_j(p) = e^{ipx_j}, \qquad 0 \le j < N, \tag{2.4}$$

with the corresponding eigenvalues

$$\lambda(p) = p^2, \qquad p \in [-\frac{N}{2}, \frac{N}{2} - 1]. \tag{2.5}$$

The collocation problem will be preconditioned by finite elements. Introducing the approximate FE operator $\hat{L}$, the preconditioned Richardson iteration is written as:

$$\bar{u}^{k+1} = \bar{u}^k - \alpha_k \hat{L}^{-1}(L_c \bar{u}^k - \bar{f}), \tag{2.6}$$

where k is an iteration index, α_k a relaxation factor and $\bar{u}, \bar{f}$ the vectors corresponding to the unknowns and source terms at the collocation points. The convergence of (2.6) is governed by the spectral radius $\rho(A)$ of the iteration operator defined by $A = I - \alpha_k \hat{L}^{-1} L_c$. The optimal value of the relaxation factor is:

$$\alpha_{opt} = \frac{2}{\lambda_{min} + \lambda_{max}}, \tag{2.7}$$

where λ_{min} and λ_{max} are the minimum and maximum eigenvalues of $\hat{L}^{-1} L_c$. An approximate estimate of the number of iterations n needed to reduce the error norm by a factor ζ is given by

$$n = -\log \zeta / R_\infty(A), \tag{2.8}$$

where $R_\infty(A) = -\log \rho(A)$ is the asymptotic rate of convergence of the iteration matrix. The spectral radius $\rho(A)$ which is involved in the error reduction process with the use of α_{opt} (Eq. (2.7)) is given by

$$\rho(A) = \frac{\lambda_{max} - \lambda_{min}}{\lambda_{max} + \lambda_{min}}. \tag{2.9}$$

In order to investigate this quantity for various preconditioners, we have to define the finite element problem more precisely.

Lagrangian linear elements, Hermite cubic elements (i.e., $Q1, P3$ in Ciarlet's notations [2]) as well as higher-order Lagrangian interpolants have their vertices at the Fourier collocation grid (2.3). However, for Lagrangian quadratics ($Q2$), mid-points are added at

$$x_{j+\frac{1}{2}} = \frac{2\pi}{N}(j + \frac{1}{2}), \qquad j \in [0, N[, \tag{2.10}$$

while for Lagrangian cubics ($Q3$), we have additional grid nodes located at

$$x_{j+\frac{1}{3}}, x_{j+\frac{2}{3}}, \qquad j \in [0, N[, \tag{2.11}$$

with obvious definitions. For the Lagrangian case, the FE unknowns are the nodal values, while for the Hermite case, the unknowns are u_j and u'_j, the prime denoting the first-order derivative of u. In [5], the iteration operator is written as:

$$A \equiv I - S_h^{-1} M_h I_h L_c, \tag{2.12}$$

2

where S_h is the stiffness matrix, M_h the mass matrix, I_h an interpolation matrix evaluating the Fourier interpolant of the collocation operator at the FE nodes. The mesh size of the FE grid is defined by

$$h = 2\pi/N.$$

For $Q1$ elements, I_h reduces to the unit matrix; for higher-order interpolants however, the structure of this matrix is more complicated. In order to avoid writing the details of I_h, we will systematically assume the use of static condensation. Consequently, the iteration operator may be written:

$$A = I - \hat{S}_h^{-1} \hat{M}_h L_c, \tag{2.13}$$

where $\hat{S}_h$ and $\hat{M}_h$ refer to stiffness and mass matrices after static condensation.

2.1. Linear Lagrangian Elements

For an interior node, the expressions for the stiffness and mass matrices are well-known:

$$S_h u_j = \frac{1}{h}(-u_{j-1} + 2u_j - u_{j+1}), \tag{2.14}$$

$$M_h f_j = \frac{h}{6}(f_{j-1} + 4f_j + f_{j+1}). \tag{2.15}$$

Fourier analysis of (2.14), (2.15) with the eigenfunction (2.4) leads to the expression of the eigenspectrum of $S_h^{-1} M_h L_c$, denoted by $\sigma(p)$,

$$\sigma(p) = \frac{(ph/2)^2}{\sin^2 ph/2} \frac{(2 + \cos ph)}{3}, \qquad -\frac{N}{2} \le p \le \frac{N}{2} - 1. \tag{2.16}$$

Typically, the second factor in the right-hand side of (2.16) comes from the contribution of the mass matrix. In the case of finite difference (FD) preconditioning, this factor is one. For $p = 0$, $\sigma(p) = 1$, while for $p = -N/2, \sigma(p) = \pi^2/12$. This last value should be compared to the FD equivalent which is $\sigma(p) = \pi^2/4$ [7]. The eigenvalue spectrum of the FE preconditioning is reduced because of the beneficial presence of the mass matrix. Fig. 1 shows the behavior of $\sigma(p)$ with respect to p for $h = 2\pi/100$. The function has a minimum value equal to 0.693. Therefore, the optimum value for α is

$$\alpha_{opt} \simeq 1.18, \tag{2.17}$$

and over-relaxation is possible for FE preconditioning unlike the FD preconditioning where under-relaxation is required to converge. In practice, the Q1 preconditioning with a spectral radius of 0.18 converges twice as fast as the FD preconditioner whose spectral radius is of the order of 0.42.

2.2. Quadratic Lagrangian Elements

The equations related to nodes j and $j \pm \frac{1}{2}$ may be cast in the following matrix form:

$$\frac{1}{3h} \begin{pmatrix} -8 & 16 & -8 & 0 & 0 \\ 1 & -8 & 14 & -8 & 1 \\ 0 & 0 & -8 & 16 & -8 \end{pmatrix} \begin{pmatrix} u_{j-1} \\ u_{j-\frac{1}{2}} \\ u_j \\ u_{j+\frac{1}{2}} \\ u_{j+1} \end{pmatrix} = \frac{h}{15} \begin{pmatrix} 1 & 8 & 1 & 0 & 0 \\ -\frac{1}{2} & 1 & 4 & 1 & -\frac{1}{2} \\ 0 & 0 & 1 & 8 & 1 \end{pmatrix} \begin{pmatrix} f_{j-1} \\ f_{j-\frac{1}{2}} \\ f_j \\ f_{j+\frac{1}{2}} \\ f_{j+1} \end{pmatrix}. \quad (2.18)$$

The use of static condensation eliminates the contribution of $u_{j-\frac{1}{2}}$ and $u_{j+\frac{1}{2}}$ and Eq. (2.18) reduces to only one relationship for node j on the collocation grid

$$\frac{1}{h}(-u_{j-1} + 2u_j - u_{j+1}) = \frac{h}{3}(f_{j-\frac{1}{2}} + f_j + f_{j+\frac{1}{2}}). \quad (2.19)$$

Let us notice that for $\hat{S}_h$ on the left hand-side of (2.19), we recover the stiffness matrix S_h associated to Q1 elements whereas in the right-hand side, $\hat{M}_h$ corresponds to a different quadrature rule. Carrying out the Fourier analysis of (2.19), one obtains

$$\sigma(p) = \frac{(ph/2)^2}{\sin^2 ph/2} \frac{1}{3}(1 + 2\cos(ph/2)), \qquad -\frac{N}{2} \le p \le \frac{N}{2} - 1. \quad (2.20)$$

For the particular values $p = 0$ and $p = -N/2$, $\sigma(p)$ is equal to 1 and $\pi^2/12$, respectively. As $\sigma(p)$ is a monotically decreasing function with respect to p (Fig. 1), the optimum value of α is

$$\alpha_{opt} = 2/(1 + \pi^2/12) = 1.0974, \quad (2.21)$$

and the corresponding spectral radius $\rho(A)$ is equal to 0.0974.

2.3. Cubic Lagrangian Elements

For the sake of compactness, we give the local stiffness and mass matrices over the uniform mesh:

$$S_h = \frac{2}{h} \begin{pmatrix} 37/20 & -189/80 & 27/40 & -13/80 \\ -189/80 & 27/5 & -297/80 & 27/40 \\ 27/J40 & -297/80 & 27/5 & -189/80 \\ -13/80 & 27/40 & -189/80 & 37/20 \end{pmatrix} \quad (2.22)$$

$$M_h = \frac{h}{2} \begin{pmatrix} 16/105 & 33/260 & -3/70 & 19/840 \\ 33/280 & 27/35 & -27/280 & -3/70 \\ -3/J70 & -27/280 & 27/35 & 33/280 \\ 19/840 & -3/70 & 33/280 & 16/105 \end{pmatrix}. \quad (2.23)$$

Assembling the matrices of (2.22), (2.23) over two adjacent elements and eliminating the four unknowns attached to the interior nodes $u_{j\pm1/3}, u_{j\pm2/3}$, we are left with the relation:

$$\frac{1}{h}(-u_{j-1} + 2u_i - u_{j+1}) = \frac{h}{10}\left(\frac{f_{j-1}}{6} + \frac{3}{4}f_{j-\frac{2}{3}} + 3f_{j-\frac{1}{3}} + \frac{13}{6}f_j + 3f_{j+\frac{1}{3}} + \frac{3}{4}f_{j+\frac{2}{3}} + \frac{f_{j+1}}{6}\right). \quad (2.24)$$

4

Here again, as in the previous case, we recover in the left-hand side of (2.24) the stiffness matrix of Q1 elements. Fourier analysis of (2.24) leads to the eigenvalue spectrum $\sigma(p)$:

$$\sigma(p) = \frac{(ph/2)^2}{\sin^2(ph/2)} \frac{1}{10} \left(\frac{4}{\sqrt{3}} \cos^3 \frac{ph}{3} + 3\cos^2 \frac{ph}{3} + 5\cos \frac{ph}{3} + \frac{2}{3} \right), \qquad -\frac{N}{2} \le p \le \frac{N}{2} - 1. \quad (2.25)$$

The particular values of $\sigma(p)$ corresponding to $p = 0$ and $p = -N/2$ are $\sigma(p) = 1$ and $49\pi^2/480 \simeq 1.007522$. The optimal value of the relaxation factor is given by $2/(1 + 49\pi^2/480) \simeq 0.9963$ and the corresponding spectral radius $\rho(A)$ is equal to 0.00375.

Looking back at the results in the previous subsections, one observes that the spectral radius $\rho(A)$ diminishes with increasing polynomial degrees. This does not mean however that one should use higher order elements in the preconditioning because they involve more computational work as the bandwidth of the algebraic system increases.

2.4. Cubic Hermite Elements

At node j, the discrete equations are

$$-\frac{6}{5h}(u_{j-1} - 2u_j + u_{j+1}) - \frac{1}{10}(u'_{j-1} - u'_{j+1}) = \frac{13h^2}{420}(f'_{j-1} - f'_{j+1})$$
$$+ \frac{h}{7}\left(\frac{9}{10}f_{j-1} + \frac{26}{5}f_j + \frac{9}{10}f_{j+1}\right), \quad (2.26)$$

$$\frac{1}{10}(u_{j-1} - u_{j+1}) - \frac{h}{30}(u'_{j-1} - 8u'_j + u'_{j+1}) = -\frac{13}{420}h^2(f_{j-1} - f_{j+1})$$
$$- \frac{h^3}{140}\left(f'_{j-1} - \frac{8}{3}f'_j + f'_{j+1}\right). \quad (2.27)$$

Fourier analyzing (2.26), one gets the spectrum:

$$\sigma(p) = \frac{(ph/2)^2}{6\sin^2(ph/2) - (ph/2)\sin(ph/2)\cos(ph/2)} \frac{1}{7}\left(26 + 9\cos ph + \frac{13}{6}ph \sin ph\right),$$
$$|ph| \in [0, \pi]. \quad (2.28)$$

For $p = 0$ and $-N/2$, $\sigma(p) = 1$ an $17\pi^2/168 \simeq 0.9987$, respectively. Fig. 1 displays the behavior of $\sigma(p)$, which is first slightly decreasing with respect to p achieving its minimum value 0.97722 and then increasing to 1. The optimal value of α is 1.01152 and the corresponding spectral radius 0.0115, an intermediate value in between those of Q2 and Q3 preconditioning.

3. HYPERBOLIC PROBLEMS

We now turn our attention to the first-order differential equation

$$u_x = f, \quad (3.1)$$

5

in the periodic case. The eigenfunctions of (3.1) are again (2.4) with the eigenvalues

$$\lambda(p) = ip, \qquad p \in [-\frac{N}{2}, \frac{N}{2} - 1].$$

3.1. Linear Lagrangian Elements

Using the standard Galerkin approach, a centered scheme is produced and yields the discrete equation

$$\frac{u_{j+1} - u_{j-1}}{2} = \frac{h}{6}(f_{j-1} + 4f_j + f_{j+1}). \tag{3.2}$$

By Fourier analysis, we obtain:

$$\sigma(p) = \frac{ph}{\sin ph} \frac{2 + \cos ph}{3}, \qquad |ph| \in [0, \pi]. \tag{3.3}$$

For $p = 0$, $\sigma(p) = 1$, while $\sigma(-N/2)$ is obviously unbounded as in the FD case. The presence of the mass matrix does not help to circumvent the difficulty.

One may proceed, however, using an upwinding technique. This has been a key step to treat hyperbolic problems. In finite elements, the method uses separate test and trial function spaces, i.e., the Petrov-Galerkin method. There are several ways to implement upwinding. Let us introduce the weight functions $w^i(r), (i = 1, 2)$ defined on the reference interval $[-1, +1]$ by Heinrich and Zienkiewicz [8]:

$$w^i(r) = \varphi^i(r) + (-1)^i \epsilon F(r), \qquad -1 \leq r \leq 1, \tag{3.4}$$

where $\varphi^i(r)$ are the linear Lagrangian trial functions, $F(r)$ an auxiliary quadratic element vanishing at both end points

$$F(r) = \frac{3}{4}(1 - r^2), \tag{3.5}$$

and ϵ the upwinding parameter to be given independently. Using φ^i and w^i as trial and test functions respectively, one gets

$$-\frac{1 + \epsilon}{2h} u_{j-1} + \frac{\epsilon}{h} u_j + \frac{1 - \epsilon}{2h} u_{j+1} = \frac{2 + 3\epsilon}{12} f_{j-1} + \frac{2}{3} f_j + \frac{2 - 3\epsilon}{12} f_{j+1}. \tag{3.6}$$

This equation reduces to (3.2) when $\epsilon = 0$ (no upwinding). With a value of ϵ as yet undefined, the Fourier analysis of (3.6) leads to complex eigenvalues given by:

$$\sigma(p) = \frac{1}{6} \frac{1}{\epsilon(1 - \cos ph) + i \sin ph}(3\epsilon ph \sin ph + 2iph(2 + \cos ph)), \qquad |ph| \in [0, \pi]. \tag{3.7}$$

For $p = 0, \sigma(p) = 1$ while for $p = -N/2, \sigma(p) = i/2$ independently of the value of ϵ. Upwinding forces the spectrum of $S_h^{-1} M_h L_c$ almost entirely inside the unit circle, as shown on Fig. 2 where the eigenvalues (3.7) have been plotted for $\epsilon = 1$. The spectral radius of the matrix A in this case is equal to $\sqrt{5}/2$ and under-relaxation is required in order to ensure convergence of the preconditioning iterations. The eigenvalues (3.7) being complex, the evaluations of α_{opt} and the spectral radius $\rho(A)$ are no longer given by (2.7) and (2.9).

6

3.2. Quadratic Lagrangian Elements

Another way to solve (3.1) consists in using a FE preconditioner based on quadratic Lagrangian elements. Applying the Galerkin approach and assembling the contributions of two adjacent elements at node j, one obtains a set of three equations related to nodes j and $j \pm \frac{1}{2}$ similar to (2.18), which are cast in matrix form:

$$
\begin{pmatrix}
-\frac{2}{3} & 0 & \frac{2}{3} & 0 & 0 \\
\frac{1}{6} & -\frac{2}{3} & 0 & \frac{2}{3} & -\frac{1}{6} \\
0 & 0 & -\frac{2}{3} & 0 & \frac{2}{3}
\end{pmatrix}
\begin{pmatrix}
u_{j-1} \\ u_{j-\frac{1}{2}} \\ u_j \\ u_{j+\frac{1}{2}} \\ u_{j+1}
\end{pmatrix}
= \frac{h}{30}
\begin{pmatrix}
2 & 16 & 2 & 0 & 0 \\
-1 & 2 & 8 & 2 & -1 \\
0 & 0 & 2 & 16 & 2
\end{pmatrix}
\begin{pmatrix}
f_{j-1} \\ f_{j-\frac{1}{2}} \\ f_j \\ f_{j+\frac{1}{2}} \\ f_{j+1}
\end{pmatrix}.
\tag{3.8}
$$

If static condensation is carried out through Gaussian elimination, the contribution of the exterior nodes u_{j-1}, u_{j+1} disappears and one is left with a staggered scheme:

$$
\frac{2}{3}(u_{j-\frac{1}{2}} - u_{j+\frac{1}{2}}) = \frac{h}{60}(-f_{j-1} + 12f_{j-\frac{1}{2}} + 18f_j + 12f_{j+\frac{1}{2}} - f_{j+1}),
\tag{3.9}
$$

for Fourier analysis. Its spectrum is given by:

$$
\sigma(p) = \frac{\frac{ph}{2}}{\sin\frac{ph}{2}} \frac{9 + 12\cos\frac{ph}{2} - \cos ph}{20}, \qquad |ph| \in [0, \pi].
\tag{3.10}
$$

It is monotonically decreasing and bounded by $\sigma(0) = 1$ and $\sigma(-N/2) = \pi/4$ as shown on Fig. 3. One should notice that the first term in the right-hand side of (3.10) is identical to the spectrum obtained in the FD case where the function is computed on the main grid while the derivative is evaluated by first-order differences on a staggered grid. The second term whose maximum value is equal to 1 is induced by the presence of the mass matrix and reduces to unity in the FD case. The optimal value of α is equal to

$$
\alpha_{opt} = 2/(1 + \pi/4) = 1.1202,
$$

and the corresponding spectral radius $\rho(A)$ is equal to 0.1202. This staggered scheme generated by Q2 elements is the key of success for FE preconditioning of Navier-Stokes problems. This excellent behavior explains the reason why in Demaret-Deville [5], the relaxation parameter was almost independent of the Reynolds number.

3.3. Advection-Diffusion Model

The last scalar model analyzed in this paper is the one-dimensional advection-diffusion problem. The differential equation writes

$$
-\kappa u_{xx} + c u_x = f(x),
\tag{3.11}
$$

where κ is the diffusion coefficient and c the constant advection velocity. Particular interest bears on advection dominated problems which impose severe conditions on the element mesh size (cfr. Thomasset [9]). With the eigenvectors (2.4), the eigenvalues of (3.11) are

$$
\lambda(p) = p^2 + \frac{i\gamma p}{h}, \qquad p \in [-\frac{N}{2}, \frac{N}{2} - 1],
$$

7

where γ is the cell Reynold's number defined by $\gamma = ch/\kappa$.

Using the linear FE basis and upwinding introduced in the previous section, one gets the discrete equations

$$-(1 + \gamma\frac{1+\epsilon}{2})u_{j-1} + (2 + \gamma\epsilon)u_j - (1 - \gamma\frac{1-\epsilon}{2})u_{j+1} = \frac{h^2}{12}[(2 + 3\epsilon)f_{j-1} + 8f_j + (2 - 3\epsilon)f_{j+1}].$$
(3.12)

where ϵ is the upwinding parameter of Eq. (3.4). With no upwinding (i.e., $\epsilon = 0$), stability requirements restrict γ to values ≤ 2. The Fourier analysis of (3.12) is straightforward. The eigenvalues of (3.12) are complex and given by:

$$\sigma(p) = \frac{\frac{(ph)^2}{3}(2 + \cos ph) + \epsilon\gamma\frac{ph}{2}\sin ph + i[\gamma\frac{ph}{3}(2 + \cos ph) - \epsilon\frac{(ph)^2}{2}\sin ph]}{2(2 + \epsilon\gamma)\sin^2\frac{ph}{2} + i\gamma\sin ph}, \quad |ph| \in [0, \pi].$$
(3.13)

In absence of upwinding, Eq. (3.13) reduces to an analytical expression whose real and imaginary parts may be written in compact form:

$$Re(\sigma(p)) = ph\frac{4ph\sin^2\frac{ph}{2} + \gamma^2\sin ph}{16\sin^4\frac{ph}{2} + \gamma^2\sin ph}\frac{2 + \cos ph}{3},$$

$$Im(\sigma(p)) = \gamma ph\frac{4\sin^2\frac{ph}{2} - ph\sin ph}{16\sin^4\frac{ph}{2} + \gamma^2\sin ph}\frac{2 + \cos ph}{3}.$$
(3.14)

The factor $(2 + \cos ph)/3$ in the right-hand side of (3.14) is another example of the contribution of the mass matrix in FE preconditioning. Like in Eq (2.16), this factor reduces to unity in the expression of the eigenvalues corresponding to FD preconditioning. One can draw similar conclusions to the diffusion problem, except for the complex nature of the eigenvalues. Introducing $ph = 0$ and $ph = \pi$ into the eigenvalues of the FD case gives the bounds of the spectrum:

$$1 \leq Re(\sigma^{FD}) \leq \frac{\pi^4}{4}, \quad 0 \leq Im(\sigma^{FD}) \leq \frac{\gamma\pi}{4}.$$
(3.15)

In the FE case, the upper bounds are reduced by a factor 3 because of the presence of the mass matrix. Figure 4 displays the result (3.14) for both FD and FE preconditionings and for two different values of γ (i.e., 0.2 and 2). Even in the limit case $\gamma = 2$, the spectrum of A for FE preconditioning lies inside the unit circle. Reducing the value of the cell Reynolds number brings the eigenvalues closer to the real axis.

Figure 5 exhibits (3.13) with $\gamma = 2$, with and without upwinding. In the upwinding case, ϵ was chosen equal to 1. The eigenspectrum is rotated counterclockwise and slightly stretched inducing a somewhat larger spectral radius.

4. STOKES EQUATIONS

Let us write the Stokes equations in stress formulation:

$$div\underline{\sigma} + \rho\underline{f} = 0,$$
(4.1)

8

$$div\,\underline{v} = 0. \tag{4.2}$$

The symbol $\underline{\underline{\sigma}}$ denotes the stress tensor, ρ is the density, $\underline{f}$ the body force term and $\underline{v}$ is the velocity field. Eq. (4.1) is the momentum equation and $\overline{E}$q. (4.2) enforces the continuity constraint. The 2-D Stokes problem may be reduced to a 1-D problem if the solution of (4.1), (4.2) is sought as a Fourier mode:

$$\underline{v} = \underline{v}(x)e^{iky}, p = p(x)e^{iky}. \tag{4.3}$$

Introducing (4.3) in (4.1), (4.2), we get:

$$-\frac{\partial p}{\partial x} + 2\mu\frac{\partial u^2}{\partial x^2} + ik\mu(iku + \frac{\partial v}{\partial x}) + \rho f_x = 0, \tag{4.4}$$

$$\mu\frac{\partial}{\partial x}(iku + \frac{\partial v}{\partial x}) - ikp - 2\mu k^2 v + \rho f_y = 0, \tag{4.5}$$

$$\frac{\partial u}{\partial x} + ikv = 0, \qquad 0 \le x \le 2\pi. \tag{4.6}$$

The velocity and pressure fields are assumed to be 2π-periodic. This 1-D problem is discretized in the x direction using Fourier series of type (2 2) for each variable. The discrete collocation equations are preconditioned by finite elements such as the $Q2-Q1$ and $Q1-P0$ elements. The FE equations come from Galerkin projection. Introducing ψ_l and φ_l the trial functions for the FE approximations of the velocity and pressure fields, respectively, such that

$$\underline{v}(x) = \sum_{l=1}^{M} \underline{v}_l \psi_l, \quad p(x) = \sum_{l=1}^{N} p_l \varphi_l, \tag{4.7}$$

the discrete FE equations are obtained by use of the divergence theorem as tool for the integration by parts with the notation $f_x = f$, $f_y = g$:

$$\sum_l [2\mu A_{jl} + \mu k^2 B_{jl}]u_l - ik\mu \sum_l C_{jl}v_l - \sum_l D_{jl}p_l = \sum_l B_{jl}f_l, \qquad 0 \le j \le M, \tag{4.8}$$

$$ik\mu \sum_l C_{jl}^T u_l + \sum_l [2\mu k^2 B_{jl} + \mu A_{jl}]v_l + ik \sum_l E_{jl}p_l = \sum_l B_{jl}g_l, \qquad 0 \le j \le M, \tag{4.9}$$

$$-\sum_l D_{jl}^T u_l - ik \sum_l E_{jl}^T v_l = 0, \qquad 0 \le j \le N. \tag{4.10}$$

In (4.8-4.10), the various matrices are defined by the relationships:

$$A_{jl} = \int \frac{\partial \psi_j}{\partial x}\frac{\partial \psi_l}{\partial x}dx, \quad B_{jl} = \int \psi_j \psi_l dx, \quad C_{jl} = \int \psi_j J\frac{\partial \psi_l}{\partial x}dx,$$

$$D_{jl} = \int \frac{\partial \psi_j}{\partial x}dx, \quad E_{jl} = \int \varphi_j \psi_l dx. \tag{4.11}$$

4.1. Q2-Q1 Elements

For this element, $M = 2N$. Carrying through the algebra involved by the quadratures (4.11) and assembling by direct stiffness the contributions of the two elements connected to node j, we obtain:

$$\frac{2\mu}{3h}(u_{j-1} - 8u_{j-1/2} + 14u_j - 8u_{j+1/2} + u_{j+1})$$

$$+\frac{\mu k^2 h}{30}(-u_{j-1} + 2u_{j-1/2} + 8u_j + 2u_{j+1/2} - u_{j+1}) - \frac{ik\mu}{6}(v_{j-1} - 4v_{j-1/2} + 4v_{j+1/2} - v_{j+1})$$

$$-\frac{1}{6}(p_{j-1} - p_{j+1}) = \frac{h}{30}(-f_{j-1} + 2f_{j-1/2} + 8f_j + 2f_{j+1/2} - f_{j+1}),$$

(4.12)

$$\frac{4\mu}{3h}(-4u_j + 8u_{j+1/2} - 4u_{j+1}) + \frac{\mu k^2 h}{30}(2u_j + 16u_{j+1/2} + 2u_{j+1}) - \frac{2ik\mu}{3}(-v_j + v_{j+1})$$

(4.13)

$$-\frac{2}{3}(p_j - p_{j+1}) = \frac{h}{30}(2f_j + 16f_{j+1/2} + 2f_{j+1}),$$

$$\frac{ik\mu}{6}(-u_{j-1} + 4u_{j-1/2} - 4u_{j+1/2} + u_{j+1}) - \frac{\mu k^2 h}{15}(-v_{j-1} + 2v_{j-1/2} + 8v_j + 2v_{j+1/2} - v_{j+1})$$

$$+\frac{2\mu}{6}(v_{j-1} - 8v_{j-1/2} + 14v_j - 8v_{j+1/2} + v_{j+1}) - \frac{ikh}{3}p_j$$

$$= \frac{h}{30}(-g_{j-1} + 2g_{j-1/2} + 8g_j + 2g_{j+1/2} - g_{j+1}),$$

(4.14)

$$\frac{2ik\mu}{3}(u_j - u_{j+1}) + \frac{8\mu}{3h}(-v_j + 2v_{j+1/2} - v_{j+1}) - \frac{2\mu k^2 h}{15}(v_j + 8v_{j+1/2} + v_{j+1})$$

(4.15)

$$-\frac{ikh}{3}(p_j + p_{j+1}) = \frac{h}{15}(f_j + 8f_{j+1/2} + f_{j+1}),$$

$$\frac{1}{6}(-u_{j-1} - 4u_{j-1/2} + 4u_{j+1/2} + u_{j+1}) + \frac{2ik}{3}(v_{j-1/2} + v_j + v_{j+1/2}) = 0.$$

(4.16)

Eqs. (4.12), (4.13) and (4.16) correspond to momentum and incompressibility relations, while (4.13) and (4.15) are the momentum equations associated to mid-node $x_{j+1/2}$. Similar expressions hold for mid-node $x_{j-1/2}$ with appropriate shifts for the indices.

Now, static condensation represents a formidable task and is greatly helped by the symbolic manipulation program. Elimination of $u_{j\pm1/2}, v_{j\pm1/2}$ leads to a matrix system of order 3.

The full Fourier solution gives the collocation matrix L_c:

$$L_c = \begin{pmatrix} -2\mu l^2 - k^2\mu & -\mu kl & -il \\ -\mu kl & -\mu l^2 - 2\mu k^2 & -ik \\ -il & -ik & 0 \end{pmatrix},$$

(4.17)

where l is the wavenumber in the x direction.

The analytical computation of $\hat{S}_h^{-1}\hat{M}_h L_c$ is performed as far as the symbolic program can handle tractable expressions. Then numerical evaluation of the eigenspectrum is done. Because of the divergence-free constraint, a zero eigenvalue is systematically obtained. In Figures 6 and 7, the eigenspectrum of $\hat{S}_h^{-1}\hat{M}_h L_c$ are plotted for two cases $k = 1$ and $k = 10$, respectively. In these two figures, the lower curve shows the same behavior as the eigenspectrum of the elliptic problem solved by Q2 elements. For $l = -N/2$, $\sigma(l)$ is equal to $\pi^2/12$. For the other curve, $\sigma(0) = 1$ and $\sigma(-N/2)$ is close to 2.07. Therefore, the optimal α value is given by

$$\alpha_{opt} = 2/(2.07 + \pi^2/12) \simeq 0.69,$$

a value close to $2/3$ obtained by Demaret-Deville [3] for a 2-D Chebyshev collocation discretization of the Stokes problem preconditioned by Q2-Q1 elements.

4.2. Q1-P0 Element

The quadratures (4.11) provide less complicated discrete equations in this case:

$$\frac{2\mu}{h}(-u_{j-1} + 2u_j - u_{j+1}) - \frac{\mu h k^2}{6}(u_{j-1} + 4u_j + u_{j+1}) + \frac{ik\mu}{2}(v_{j+1} - v_{j-1})$$

$$-p_j + p_{j+1} = \frac{h}{6}(f_{j-1} + 4f_j + f_{j+1}),$$

(4.18)

$$\frac{ik\mu}{2}(u_{j-1} - u_{j+1}) - \frac{\mu k^2 h}{3}(v_{j-1} + 4v_j + v_{j+1}) + \frac{\mu}{h}(-v_{j-1} + 2v_j - v_{j+1})$$

$$-\frac{ikh}{2}(p_j + p_{j+1}) = \frac{h}{6}(g_{j-1} + 4g_j + g_{j+1}),$$

(4.19)

$$-u_{j-1} + u_{j+1} + \frac{ikh}{2}(v_{j-1} + 2v_j + v_{j+1}) = 0.$$

(4.20)

Obviously, this element generates second-order differences for partial derivatives. When the mass matrix is involved, the standard weighted mean between three adjacent nodes appears in the expressions. No static condensation is needed in this case. Fourier analyzing Eqs. (4.18)-(4.20), the stiffness and mass matrices are now:

$$S_h = \begin{pmatrix} 8\frac{\mu}{h}\sin^2(\frac{hl}{2}) + \frac{hk^2 l\mu}{3}(2 + \cos hl) & \mu k \sin hl & 2i\sin(\frac{hl}{2}) \\ \mu k \sin hl & 4\frac{\mu}{h}\sin^2(\frac{hl}{2}) + \frac{2\mu k^2 h}{3}(2 + \cos hl) & ikh\cos(\frac{hl}{2}) \\ 2i\sin hl & ikh(1 + \cos hl) & 0 \end{pmatrix},$$

$$M_h = diag(\frac{h}{3}(2 + \cos hl), \frac{h}{3}(2 + \cos hl), 0).$$

(4.21)

In Figures 8 and 9, the eigenspectrum of $S_h^{-1}M_h L_c$ are displayed for $k = 1$ and 10, respectively. In these two figures, the top curve is that of the elliptic model preconditioned by Q1 element. The bottom curve starts from 1 for $l = 0$, decreases till a minimum value close to 0.49 and then increases to reach $\sigma(-N/2) = 0.5$. The optimum value is

$$\alpha_{opt} = 2/(1 + 0.5) = 4/3.$$

11

5. CONCLUSIONS

In this paper, we have Fourier analyzed the eigenspectrum of the iteration operator for finite element preconditioning of Fourier collocation applied to one-dimensional problems. For elliptic models, this theoretical analysis confirms previous numerical findings, especially the beneficial presence of the mass matrix which reduces the bounds of the eigenspectrum. For first-order problems, linear elements without and with upwinding are considered. With quadratic elements, a staggered scheme is produced. Its eigenspectrum is bounded and ranges between 1 and $\pi/4$. Finally, a Stokes problem is reduced to a one-dimensional approach. Two types of elements are examined. The Q2-Q1 element leads to an optimum value of the relaxation parameter close to the value obtained by numerical analysis of preconditioned Chebyshev collocation. For Q1-P0 element, the method can be over-relaxed.

ACKNOWLEDGMENTS

References

[1] C. CANUTO, M. Y. HUSSAINI, A. QUARTERONI, and T. A. ZANG, *Spectral Methods in Fluid Dynamics*, Springer-Verlag, New York, 1988.

[2] P. G. CIARLET, *The Finite Element Method*, North Holland, Amsterdam, 1979.

[3] P. DEMARET and M. O. DEVILLE, "Chebyshev pseudospectral solution of the Stokes equations using finite element preconditioning," J. Comput. Phys., 83, 463, 1989.

[4] P. DEMARET and M. O. DEVILLE, "Chebyshev collocation solutions of the Navier-Stokes equations using multi-domain decomposition and finite element preconditioning," submitted to J. Comput. Phys.

[5] M. DEVILLE and E. MUND, "Chebyshev pseudospectral solution of second-order elliptic equations using finite element preconditioning," J. Comput. Phys., 60, 517, 1985.

[6] M. O. DEVILLE and E. H. MUND, "Finite element preconditioning for pseudospectral solutions of elliptic problems," SIAM J. Sci. Statist. Comput., 12, March 1990.

[7] P. HALDENWANG, G. LABROSSE, S. ABBOUDI, and M. O. DEVILLE, "Chebyshev 3-D spectral and 2-D pseudospectral solvers for the Helmholtz equation," J. Comput. Phys., 55, 115, 1984.

[8] J. C. HEINRICH and O. C. ZIENKIEWICZ, "The finite element method and upwinding techniques in the numerical solution of convection dominated flow problems" in "Finite Element Methods for Convection Dominated Flows," T. J. R. Hughes, Ed., ASME, New York, 105, 1979.

[9] F. THOMASSET, *Implementation of Finite Element Methods for Navier-Stokes Equations*, Springer-Verlag, New York, 1981.

[10] S. WOLFRAM, 'SMP, *A Symbolic Manipulation Program: Reference Manuel' Inference Corporation*, Los Angeles, California, 1983.
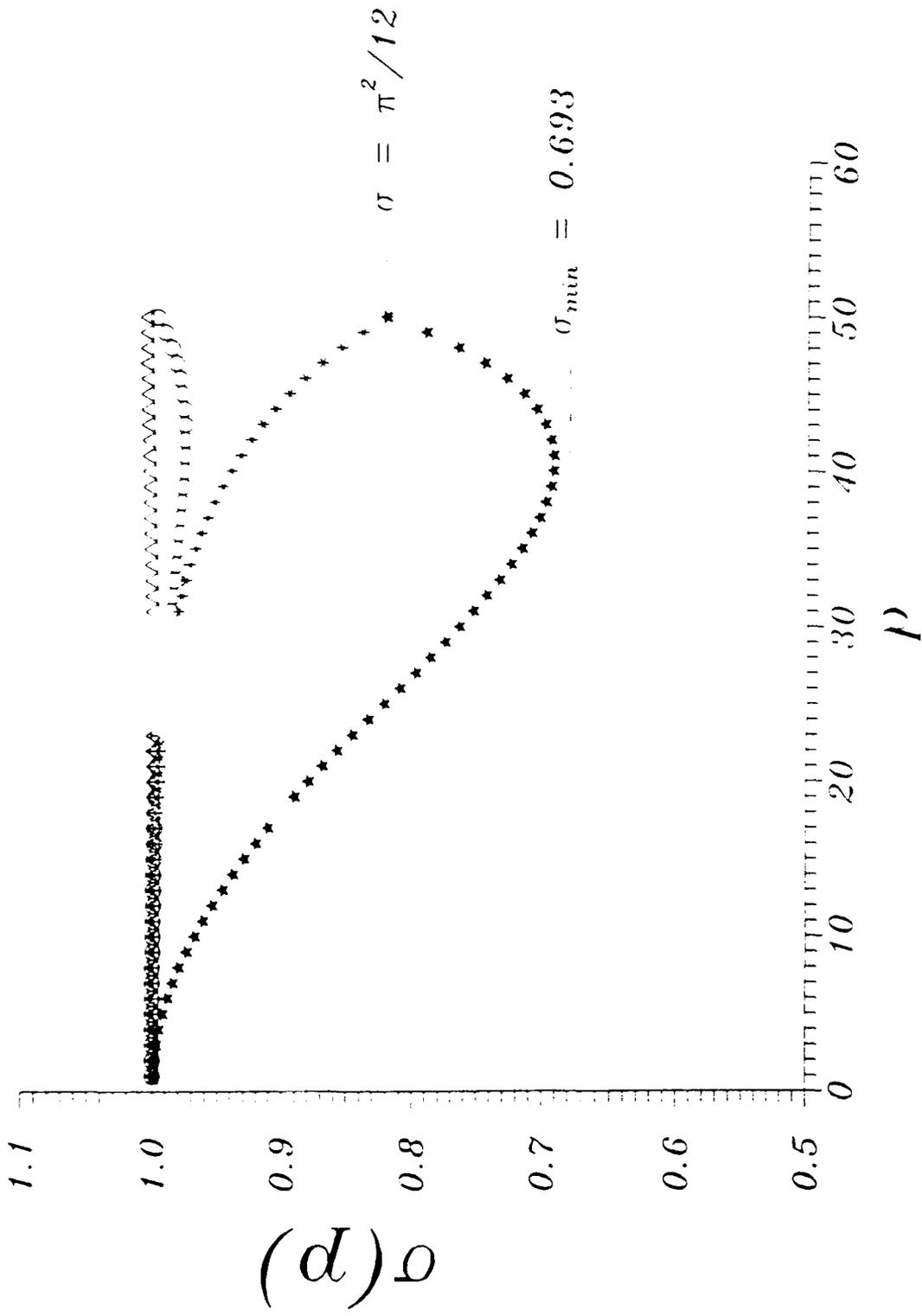
Figure 1. Eigenspectrum of $\hat{S}_h^{-1}\hat{M}_h L_c$ for an elliptic model. Preconditioners: Q1:*; Q2:*; Q3:△; Cubic Hermite: ○.
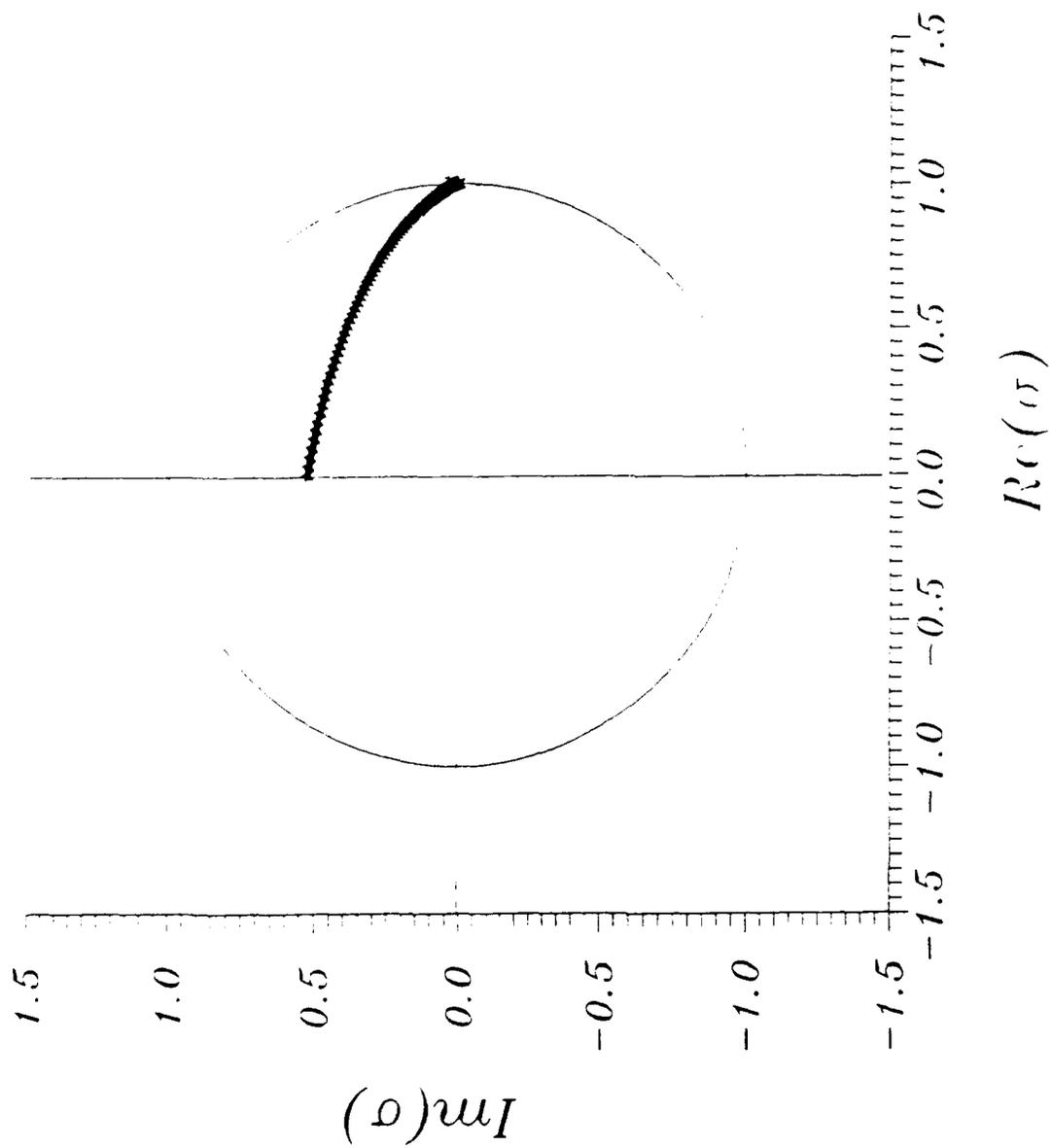
Figure 2. Eigenspectrum of $\hat{S}_h^{-1}\dot{M}_h L_c$ for a first-order operator. Upwinding with a parameter $\epsilon = 1$ is used.

15
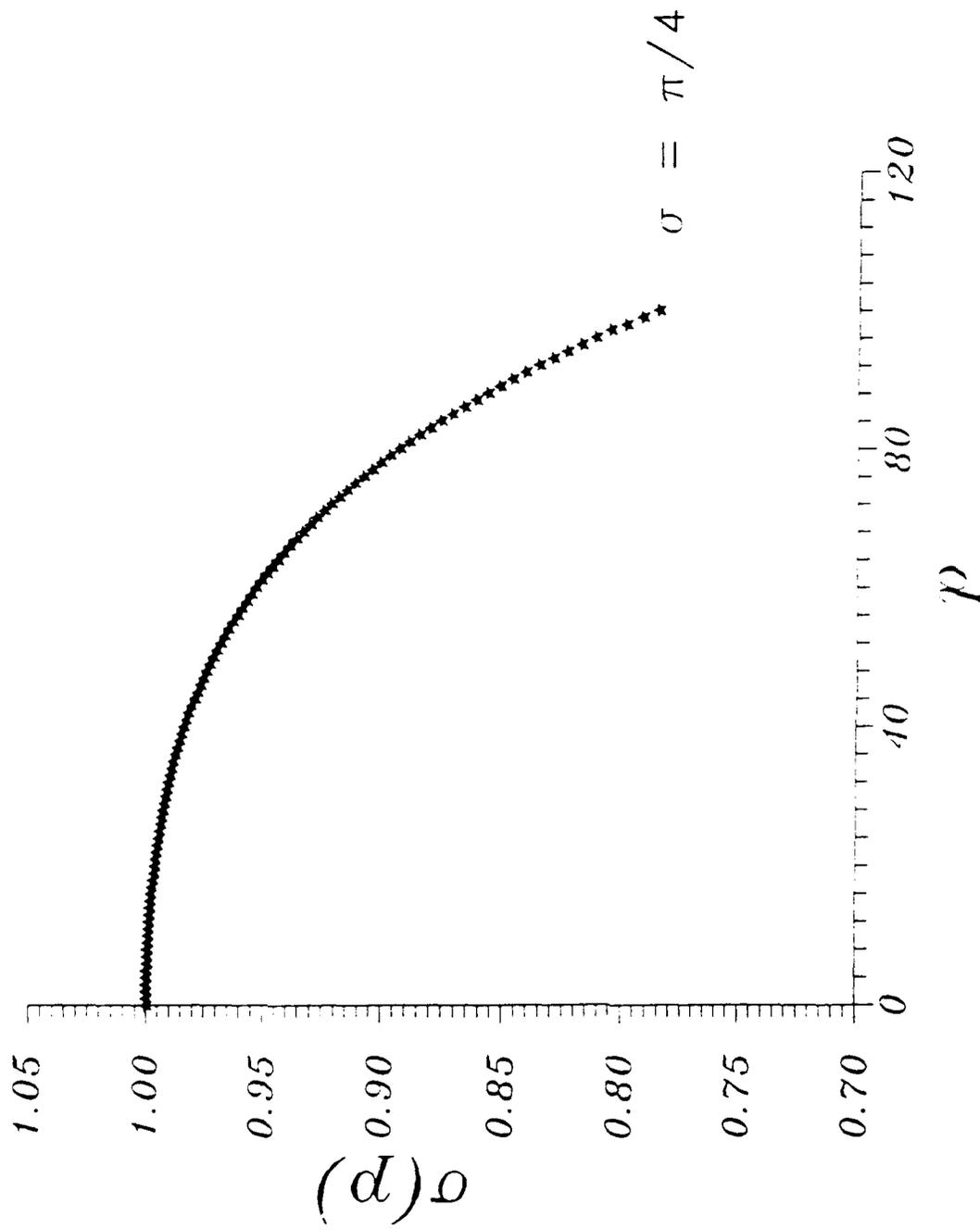
Figure 3. Eigenspectrum of a first-order operator preconditioned by Q2 elements.
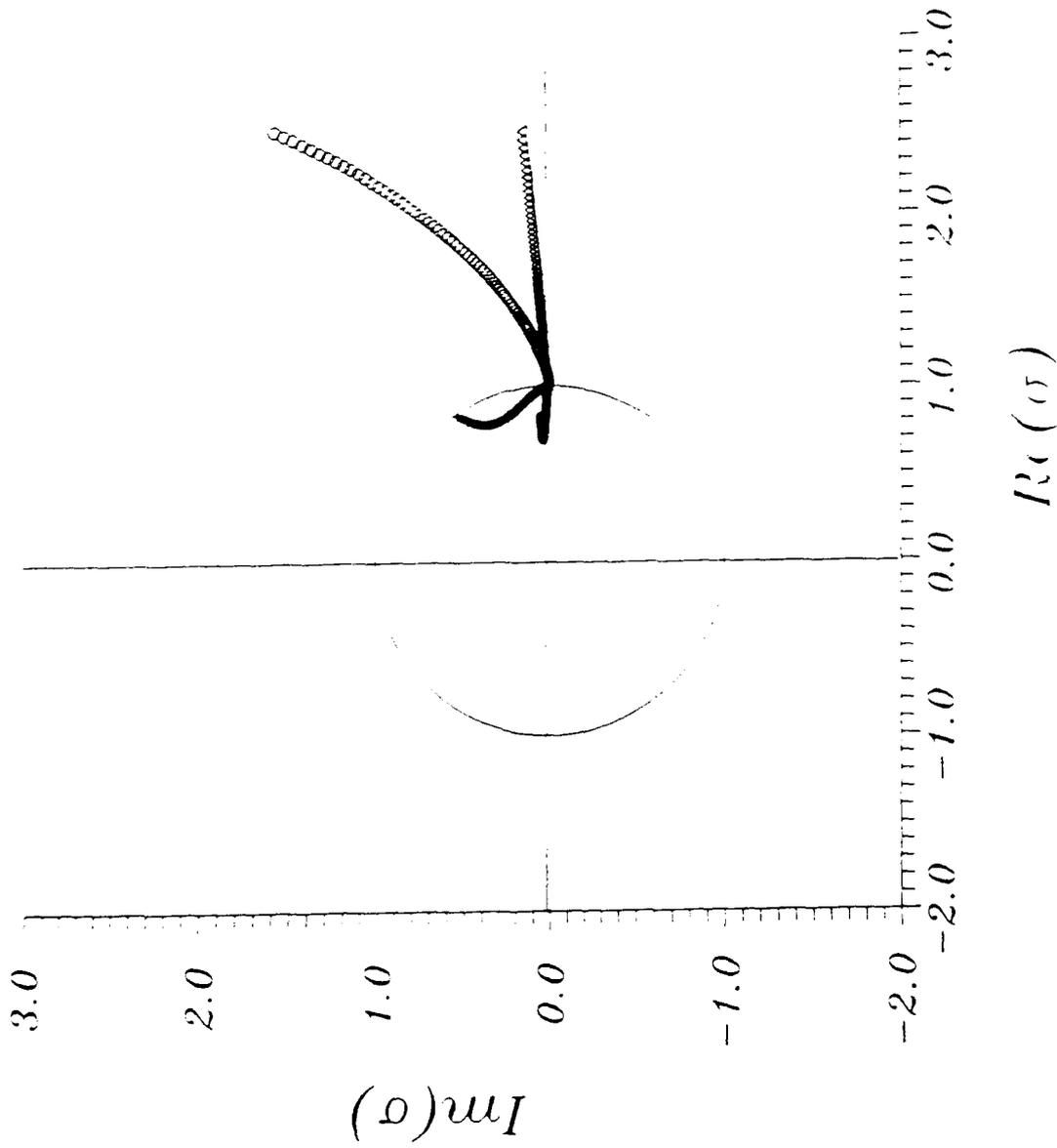
Figure 4. Eigenspectrum of an advection-diffusion problem. The curves outside the unit circle are concerned with FD preconditioning while the inside curves are related to FE preconditioning. Both top curves are obtained for the cell Reynolds number $\gamma = 2$. The bottom curves are gotten for $\gamma = 0.2$.
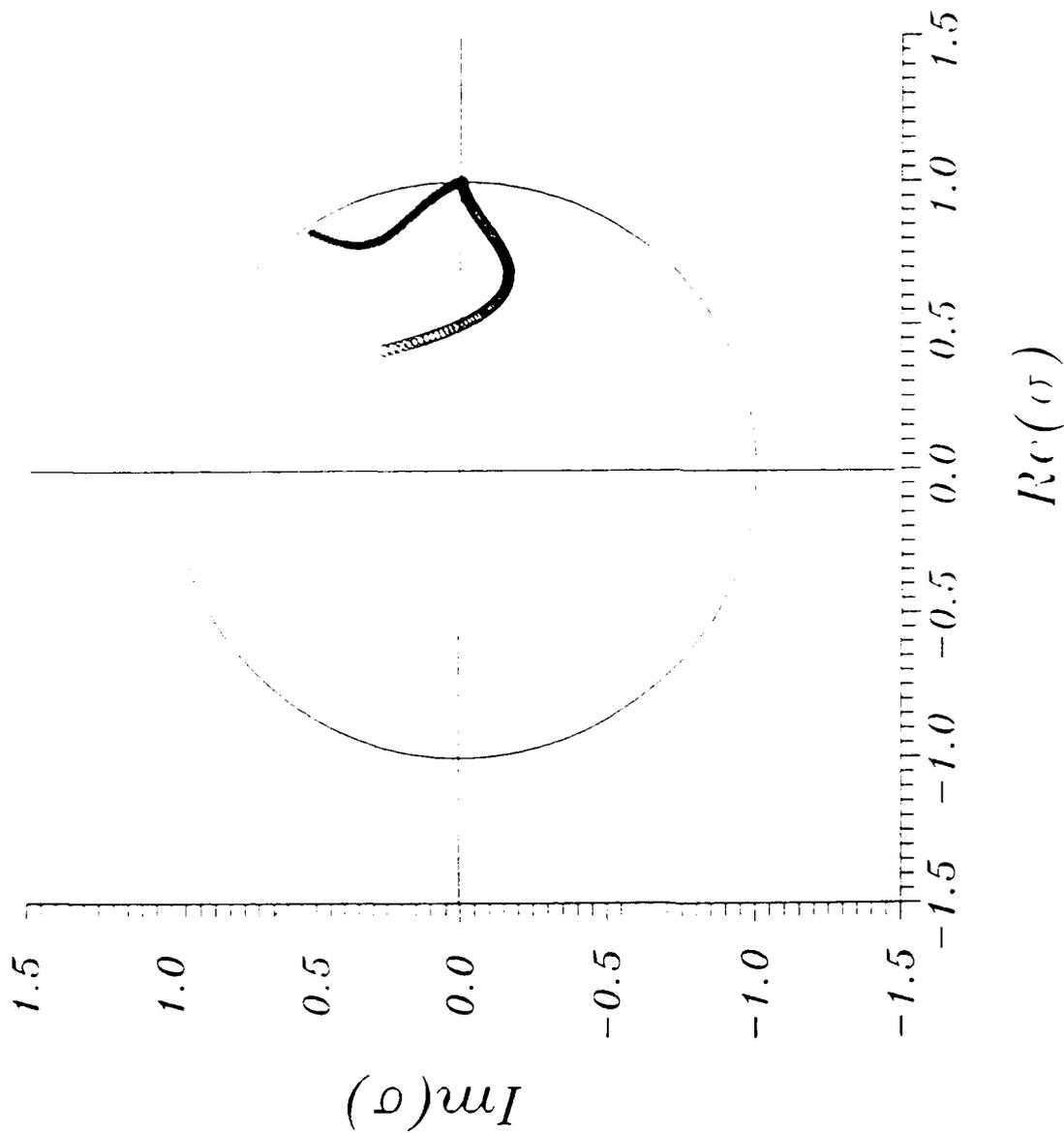
Figure 5. Eigenspectrum of the advection-diffusion problem preconditioned by Q1 elements for $\gamma = 2$, with ($\bigcirc$) and without (*) upwinding. The upwinding parameter is $\epsilon = 1$.

18
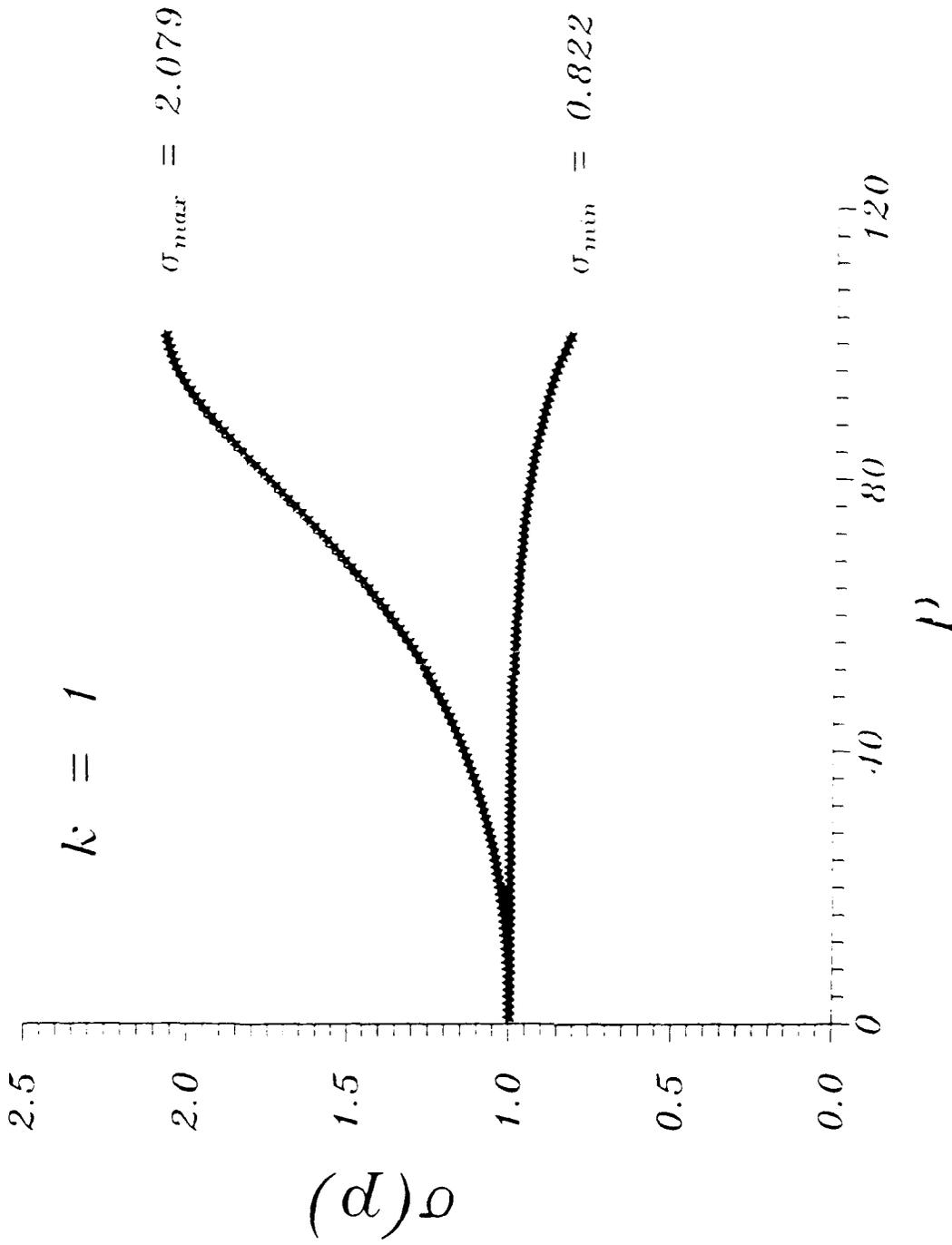
**Figure 6.** Eigenspectrum of the Stokes problem preconditioned by Q2-Q1 element. Here, $k = 1$.
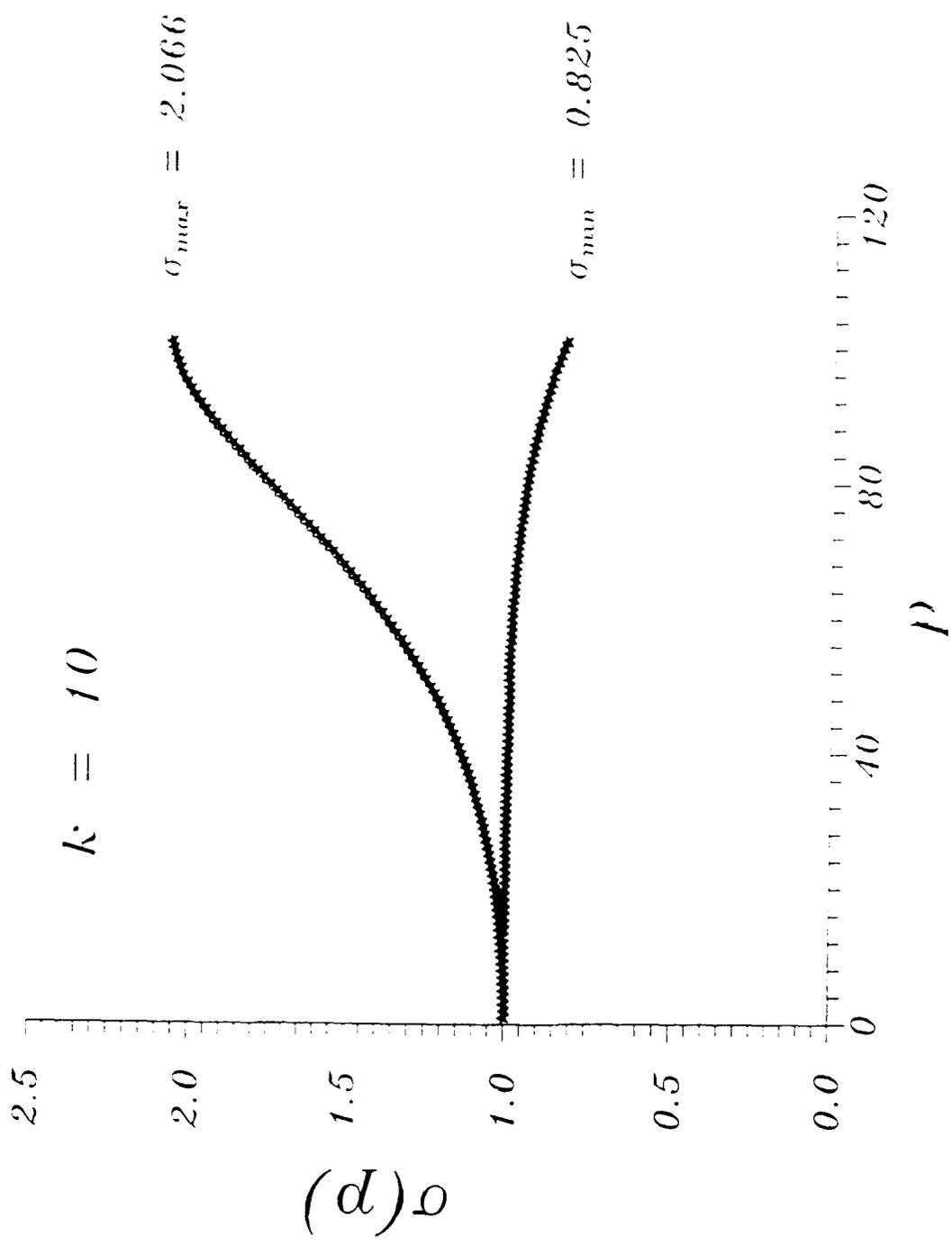
Figure 7. Same caption as Figure 6, with $k = 10$.
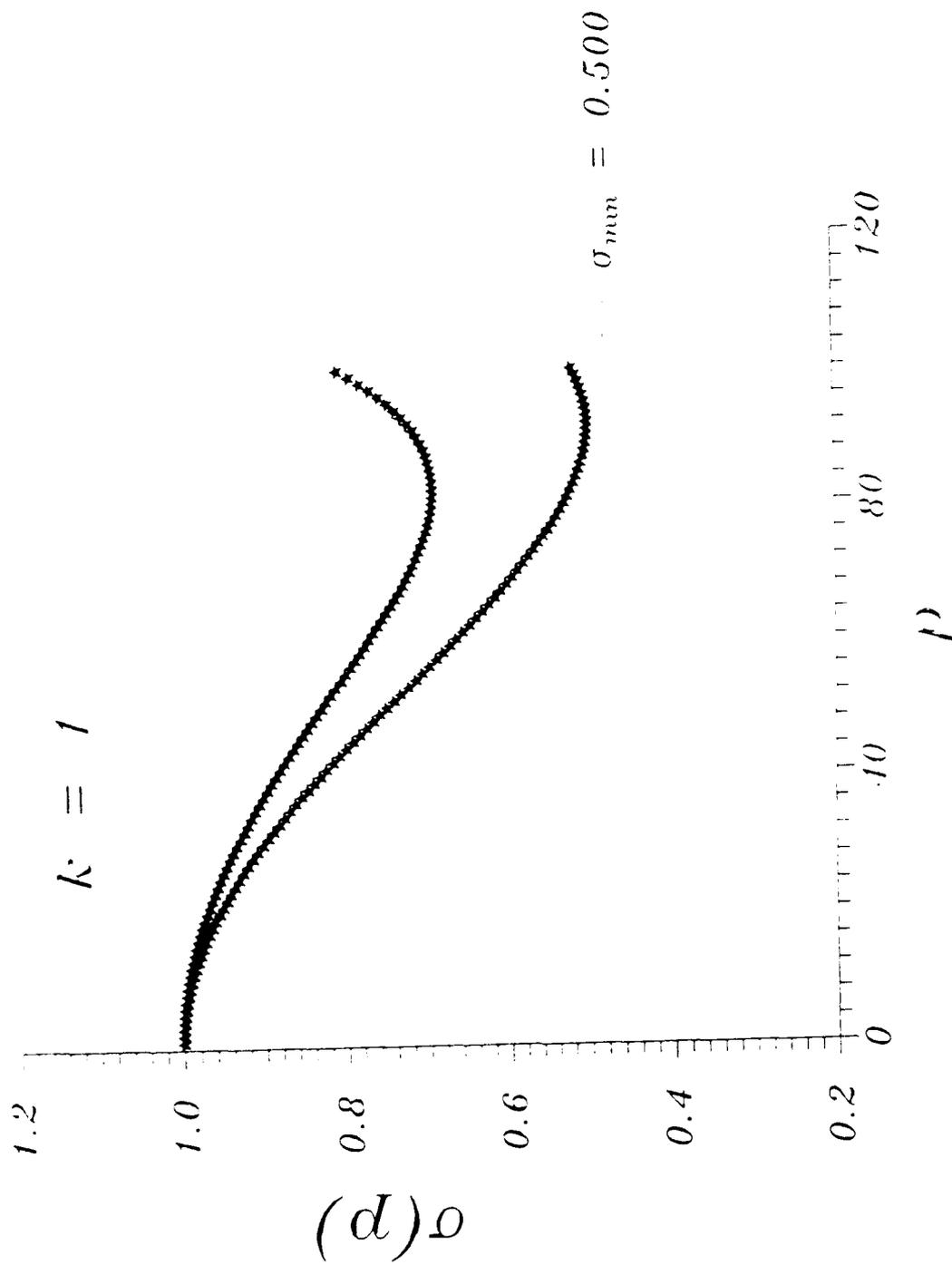
Figure 8. Eigenspectrum of the Stokes problem preconditioned by Q1-P0 element. Here, $k = 1$.
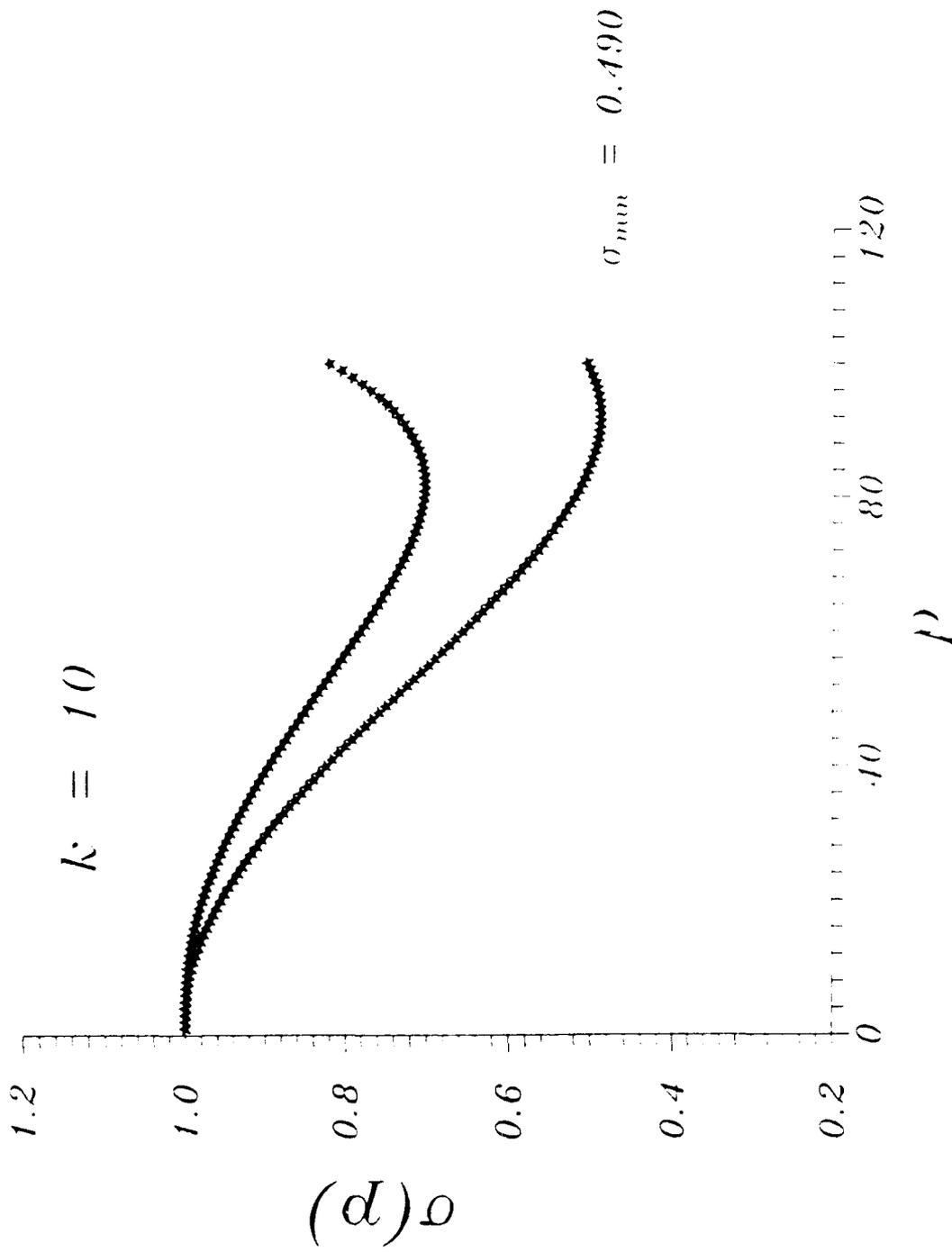
Figure 9. Same caption as Figure 8, but with $k = 10$.

NASA

National Aeronautics and Space Administration

Report Documentation Page

1. Report No. NASA CR-182040 ICASE Report No. 90-35	2. Government Accession No.	3. Recipient's Catalog No.

| 4. Title and Subtitle FOURIER ANALYSIS OF FINITE ELEMENT PRECONDITIONED COLLOCATION SCHEMES | 5. Report Date May 1990 |
| | 6. Performing Organization Code |

| 7. Author(s) Michel O. Deville Ernest H. Mund | 8. Performing Organization Report No. 90-35 |
| | 10. Work Unit No. 505-90-21-01 |

| 9. Performing Organization Name and Address Institute for Computer Applications in Science and Engineering Mail Stop 132C, NASA Langley Research Center Hampton, VA 23665-5225 | 11. Contract or Grant No. NAS1-18605 |
| | 13. Type of Report and Period Covered Contractor Report |

| 12. Sponsoring Agency Name and Address National Aeronautics and Space Administration Langley Research Center Hampton, VA 23665-5225 | 14. Sponsoring Agency Code |

16. Abstract

This paper investigates the spectrum of the iteration operator of some finite element preconditioned Fourier collocation schemes. The first part of the paper analyses one-dimensional elliptic and hyperbolic model problems and the advection-diffusion equation. Analytical expressions of the eigenvalues are obtained with use of symbolic computation. The second part of the paper considers the set of one-dimensional differential equations resulting from Fourier analysis (in the tranverse direction) of the 2-D Stokes problem. All results agree with previous conclusions on the numerical efficiency of finite element preconditioning schemes.

| 17. Key Words (Suggested by Author(s)) finite element, collocation method, eigenvalue analysis, spectral methods | 18. Distribution Statement 64 - Numerical Analysis 34 - Fluid Mechanics and Heat Transfer Unclassified - Unlimited |

| 19. Security Classif. (of this report) Unclassified | 20. Security Classif. (of this page) Unclassified | 21. No. of pages 24 | 22. Price A03 |